CHAPTER 4

Thermal Contraction Polygons and Formation of Polygonal Fracture Patterns

In periglacial environments of the Earth and Mars, polygonal patterns with an intra-polygon diameter in the range of several meters to tens of meters are observed frequently. While the formation of the terrestrial features is reasonably understood and is attributed to thermal contraction processes of the upper surface layer, Martian landforms can not be unambiguously attributed to such processes. Although most of such polygons are morphologically comparable to terrestrial ones and are therefore considered to be caused by thermal stresses, alternatives cannot be ruled out. The following sections will discuss formation of terrestrial thermal contraction patterns and summarize work on Mars. Detailed investigations have been conducted when high-resolution data became available in the late 1990s when the Mars Orbiter Camera onboard Mars Global Surveyor started its mapping phase, consequently this results in relatively few publications on this topic.

4.1. Terrestrial Polygons and Landforms

Periglacial ground on Earth is often characterized by more or less regular networks of polygonally shaped fracture patterns (figures 4.1, 4.3). These features have been investigated for nearly two centuries starting with work from *M. F. Adams (1815), A. T. von Middendorf (1867)* and *A. von Bunge (1884)* (all as cited in *Cailleux* (1971) and *Embleton and King* (1975)). It has become clear that these polygons are built up by interconnecting fractures that are caused by thermal stresses in perennially frozen ground. Such fractures form through thermal contraction of the ground in periglacial environments and provide evidence for permafrost occurrence in the subsurface in cases where these cracks are filled with ice.

Fractures propagate laterally and can form polygonal cells delineated by other fractures. These cells vary in diameter from a few decimeters up to a few meters and more; fractures usually reach a depth of several decimeters but rarely exceed 10 m (*Black*, 1976; *French*, 1996). The vertical size of individual fractures depends largely on the climatic regime and input of water/ice or sand as well as a variety of other factors discussed below that also control the shape of individual polygons.

The occurrence of polygonally shaped fracture patterns, however, does not necessarily imply that ice wedges or ice veins must be present. Consequently, ice-wedge formation is split up into two processes: frost-cracking (section 4.1.1) and wedge formation (section 4.1.2). While for epigenetic ice wedges the depth usually does not exceed the fracture depth, initial fractures can grow considerably when they are filled with ice and sediments in the case of syngenetic ice-wedge formation that reach a maximum depth of

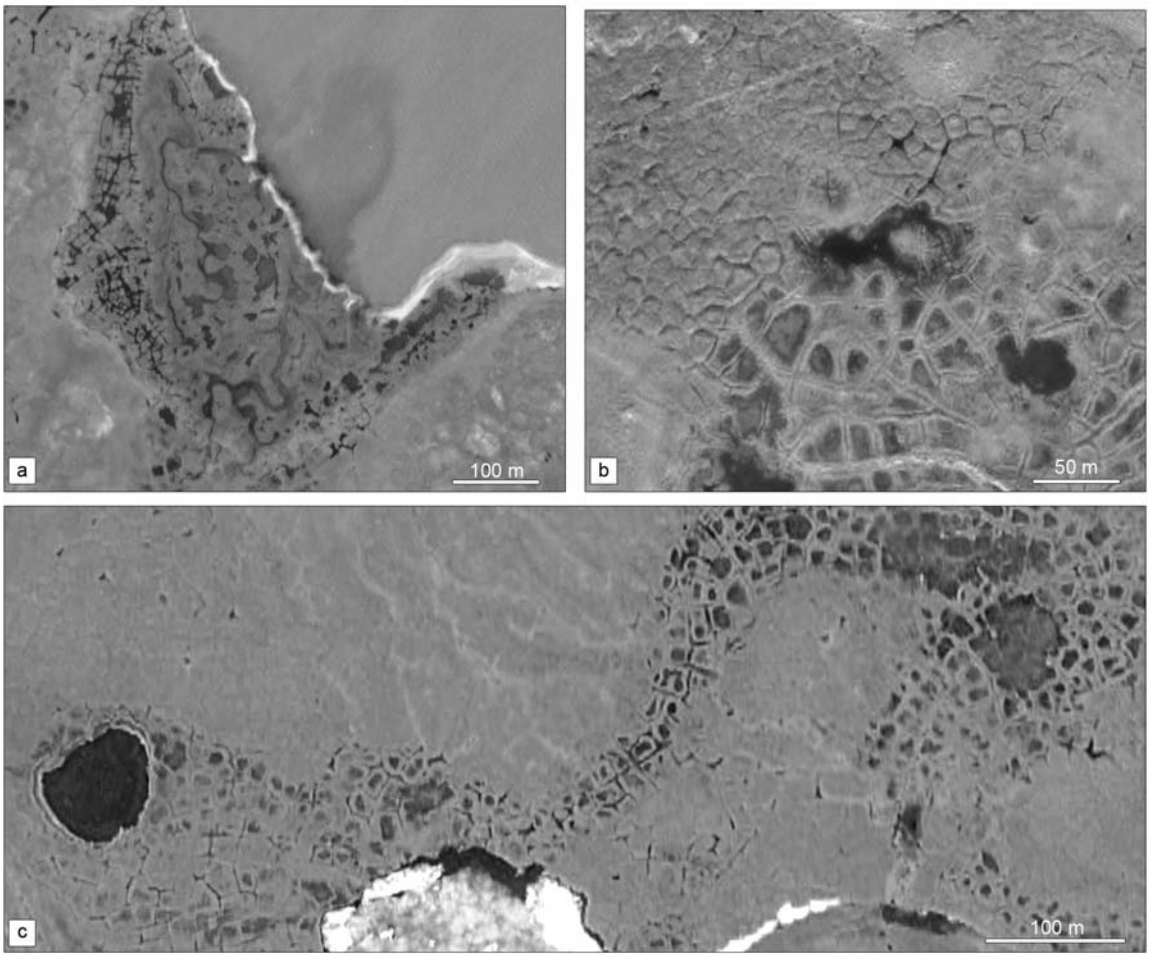

Figure 4.1.: Samples of terrestrial polygonal terrain in periglacial areas of Canada and Siberia; [a-b] Canadian high arctic, [a] oriented orthogonal networks at a shoreline, [b] irregular hexagonal double–rim polygons (lower right) and water–filled hexagonal forms (upper left), location 132.37°W, 69.73°N, [c] river plains in Siberia, oriented orthogonal and hexagonal polygonal patterns, location 111.69°E, 73.13°N. North is up in all scenes, QuickBird image data.

up to 80 m and more (*Yershov*, 2004, p- 322f). Formation of ice wedges allow constraining past or recent climatic conditions. They only form in active permafrost with surface-air temperatures well below 0°C (*French*, 1996; *Péwé*, 1966) and are also controlled by the size fraction of the sediment (*Romanovskii* (1985) as cited in *French* (1996)).

4.1.1. Frost-Cracking Process

Lowering of soil temperatures leads to thermal contraction of the ground and, consequently, formation of fissures and cracks. Water is known to reach its highest density at +4°C and starts to expand as soon as ice is formed but it contracts at temperatures below freezing in the way many surfaces materials contract when they are exposed to temperatures below 0°C. The amount of contraction is expressed usually by the coefficient of volume expansion β following

$$\Delta V = \beta \cdot V_0 \Delta T \tag{4.1}$$

$$\beta = \frac{1}{V}\left(\frac{\partial V}{\partial T}\right) \tag{4.2}$$

$$\beta = -\frac{1}{\rho}\left(\frac{\partial \rho}{\partial T}\right) \tag{4.3}$$

and for the coefficient of linear expansion α following

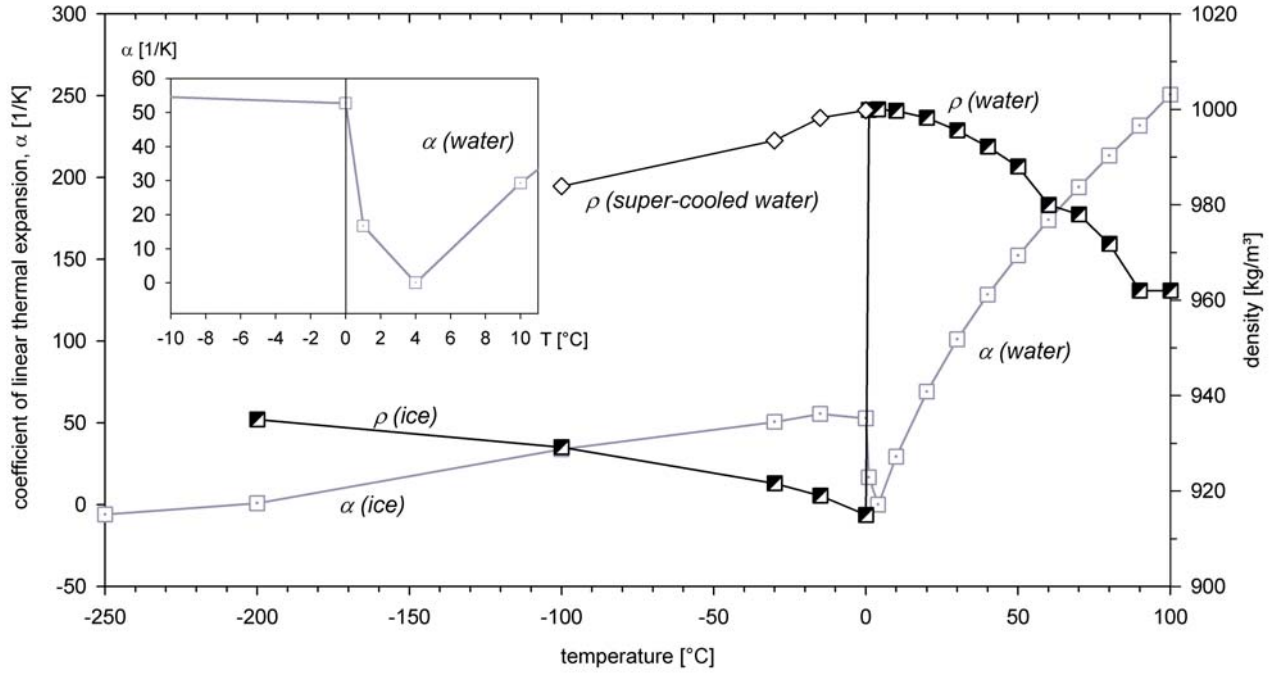

Figure 4.2.: Temperature T (°C) vs. coefficient of linear thermal expansion α (1/K) of water, super-cooled water and ice vs. density ρ (kg/m³); compilation by author on the basis of *Powell* (1958); *Butkovich* (1959); *LaPlaca and Post* (1960); *Eisenberg and Kauzmann* (1969); *Hobbs* (1975); *Cox* (1983); *Lide* (2003).

$$\Delta L = \alpha \cdot L_0 \Delta T \tag{4.4}$$

$$\alpha = \frac{1}{L}\frac{\partial L}{\partial T} \tag{4.5}$$

with ΔV and ΔL being the change of volume and length, respectively, ΔT is the change of temperature and V_0 and L_0 are the initial volume and initial length, respectively, ρ is the density of the material (*Incropera and DeWitt*, 2001). Coefficients for linear and volume expansions for isotropic material are related to each other by $\beta = 3\alpha$. Typical mean values for water ice are $\alpha = 52.7 \times 10^{-1}$ at 0°C and $\alpha = 50.5 \times 10^{-1}$ at -30°C (*Lachenbruch*, 1962) and it is considered that ice-rich soils react only little different from pure ice (*French*, 1996, p. 39).

The temperature-dependent coefficient of linear expansion decreases rapidly until a temperature of 4° is reached when the density of water has reached a maximum value. Further lowering of temperatures causes the linear expansion coefficient to increase rapidly again, i.e., the material's volume increases. When ice is formed at ~ 0°C, the coefficient decreases again and ice starts to contract as the density increases (figure 4.2). According to several laboratory experiments as cited by *Lachenbruch* (1962), p. 9ff, values for the tensile strength of soils are between 5 bar and 20 bar, although larger values of up to >30 bar have been found also and experiments have shown that the tensile strength of soils could even exceed the strength of pure ice and could become even larger if temperature decreases. This means, that an ice-wedge usually has a lower tensile strength than the frozen active layer above that wedge. *Lachenbruch* (1962) estimated the relation between temperature and stress and concluded that the relation is expressed by

$$\tau(t) \approx 3.6(2\tilde{\eta}\alpha\Delta T)^{1/3} \tag{4.6}$$

with $\tau(t)$ being the stress as a function of time, η being the viscoelastic parameter for polycrystalline ice which depends on temperature, α is the coefficient of linear expansion and ΔT is the deviation of temperature from the mean annual temperature (*Lachenbruch*, 1962, p. 17ff). Depending on η and the rate of

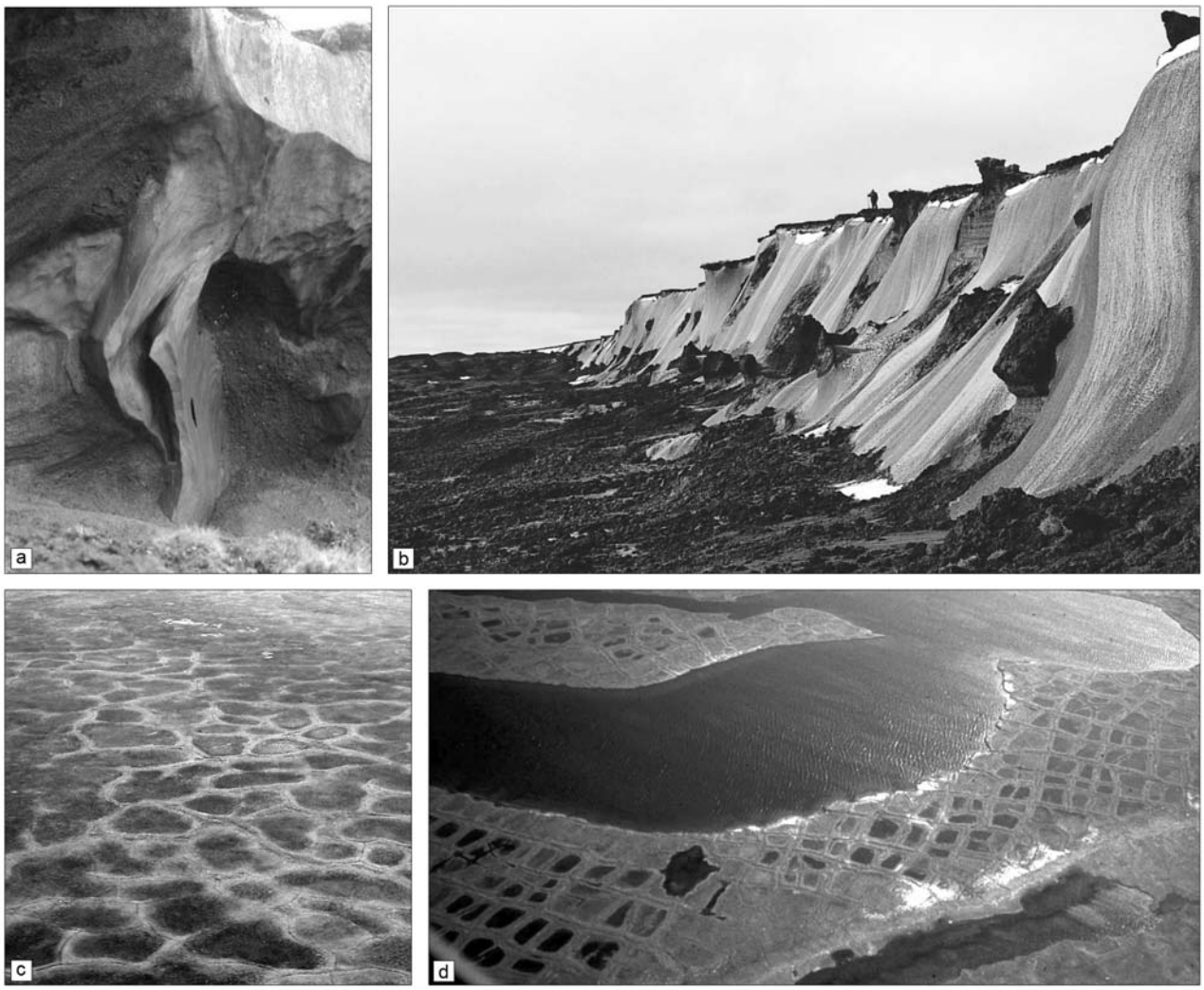

Figure 4.3.: Terrestrial ice wedges and polygonal terrain; [a] cross-section of ice wedge, Yukon Territories, approximately 3 m vertical height; [b] ice wedges at the shore of the Laptew Sea (M. Grigorjev, AWI); [c] oblique view of polygonal ground, Yukon Territories, Canadian Soil Information System (http://sis2.agr.gc.ca/cansis/); [d] oblique view of water-filled low-center polygons at the Lena Delta, Siberia (V. Rachold, AWI).

cooling, thermal stresses can reach values between 7.3 bar and 15.7 bar at the surface and 3.4 bar and 7.3 bar at the top of permafrost (*Lachenbruch*, 1962, p. 20).

From extensive field work performed under the lead of J. R. MacKay (e.g., *Mackay*, 1974, 1980, 1986, 1992) in the Canadian Mackenzie Delta region during the last 30 years data has been collected and the processes involved in formation of frost cracks and ice-wedges are fairly well understood.

In contrast to earlier suggestions by *Lachenbruch* (1962), it is now relatively clear that frost cracking usually occurs during the end of winter and is not necessarily related to extreme temperature drops but to favourable conditions defined through lowering of temperature at rates of a few degrees per day (~1.8°C/d - ~6°C/d (*Fortier and Allard*, 2005)) and the presence of an insulating cover of snow to maintain large stresses. However, frost cracking can and does occur without insulating snow cover if rates of temperature drops are large enough (*Washburn et al.* (1963) as cited in *Embleton and King* (1975), p. 42).

90% of temperature fluctuations in permafrost oc-

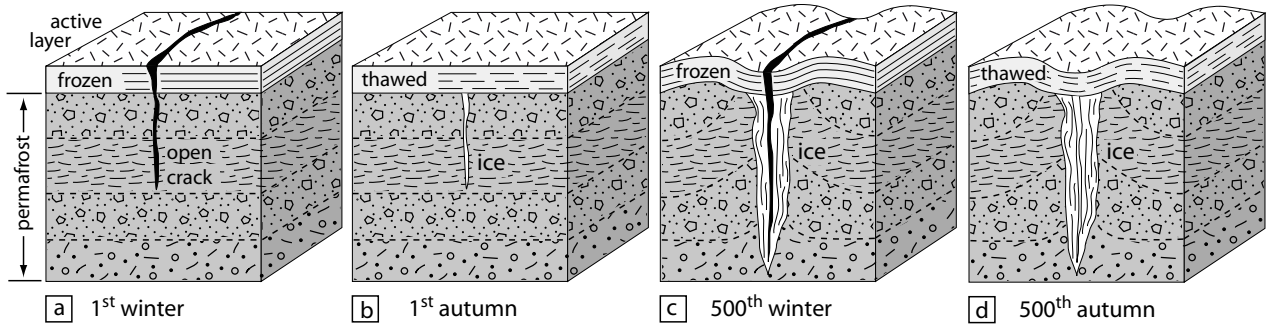

Figure 4.4.: Fracturing process and subsequent formation of stratified ice wedges through repeated freeze-thaw cycles; displaced sediments bend upwards, based on *Lachenbruch* (1962).

cur in the upper 10-20 m of permafrost; below that region, temperatures are fairly stable (*Lachenbruch*, 1966). Consequently, cracking occurs at the top of permafrost – or at the base of the insulating *active layer* – rather than at the depth of permafrost. This process was observed in the field and it explains why repeated cracking and re-activation of cracks can occur. Re-acitvation of cracks would be impossible if cracks initiated in the active layer and commence downwards, however, once a crack has formed at the permafrost boundary, it propagates upwards through the active layer as well as downwards into the permafrost (*French*, 1996, p. 92).

Such contraction cracks form natural flaws that can easily be opened again during seasons where thermal stresses exceed the material's strength. Based upon terrestrial research there are some indicators that less than half of the ice wedges are reactivated annually and therefore it is not possible to infer the age of cracks or growth rates for crack formation on the basis of the size (*Mackay*, 1986, 1992).

However, as shown by several authors, polygonal networks are still valuable indicators to obtain a rough estimate of the duration (*Black*, 1974; *Johnson*, 1990; *Williams*, 1994; *Vandenberghe et al.*, 2004) and temperature conditions (*Isarin*, 1997; *Renssen and Isarin*, 2001). Experiments and theory have provided inconsistent values for growth rates of ice wedges ranging from 1-2 mm/a (e.g., *Leffingwell* (1919), *Tumel* (1979) as cited in *Mackay* (1986)) up to 35 mm/a (*Mackay*, 1986).

4.1.2. Wedge-Formation

After initial formation of frost fissures and cracks, subsequent re-activation of cracks can cause growth in lateral and vertical direction if material is transported into the opened fissures and prohibits closure of cracks. Commonly, this infill is seasonal melt water from the upper active layer which fills the crackand freezes forming an ice vein. Such an ice vein can then be re-opened in subsequent years allowing new meltwater to percolate into the crack. Many years of re-opening, infilling and freezing produce forms known as ice wedges (figures 4.3a-b, 4.4, 4.5). According to *Leffingwell* (1915), fractures do not open more than 8-10 mm during one winter. If no moisture is available or if temperatures are not favourable (*Romanovskii* (1985) as cited in *French* (1996)), windblown sediments such as sand or soil, can intrude and form sand- or soil wedges, respectively. Thus, the occurrence of fracture patterns and polygonal networks does not necessarily mean that subsurface ice is involved in their formation. Sand wedges have been described from Antarctica (*Péwé*, 1959) and from other predominantly arid locations which receive less than 100 mm/a of precipitation (*Nichols*, 1966; *Pissart*, 1968; *French*, 1996).

Sand wedges are often composed of loess material of silt-size fraction and reach a depth of several meters (*Murton and French*, 1993). Soil wedges seem to be

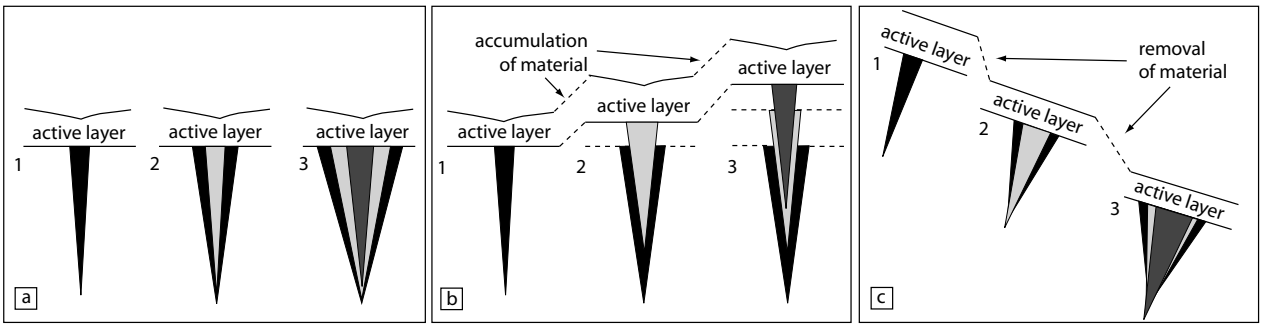

Figure 4.5.: Development of epi-, syn-, and anti-syngenetic ice wedges in terrestrial permafrost, [a] epigenetic growth, vertical and lateral growth of ice wedges by recurring fracturing and flaws; [b] growth of syngenetic wedges during accumulation of sediment, thus causing upward growth; [c] anti-syngenetic downward growth of ice wedges caused by contemporary removal of material, after *Mackay* (1990).

more frequent and their infill is connected to material from the seasonally thawed active layer (e.g., *Dylik*, 1966; *Jahn*, 1983). They develop in more continental climates and have been reported from Yakutia, Iceland, Svalbard and Scandinavia mainly. Their formation and the way material is incorporated is still not solved (*French*, 1996). Some authors suggest that they form so-called ice-wedge pseudomorphs, i.e., they form after ice-wedges thawed and the resulting open crack could be filled with soil from the active layer. Characteristic of ice-, sand- or soil wedges are a vertical stratification of the wedge caused by repeated cracking and lateral growth (figures 4.4, 4.5a-c). If there is no accumulation of sediments ontop of the active layer during subsequent seasons, the wedge will predominantly grow in lateral direction, thus forming an epigenetic wedge. The situation becomes more complicated if sediments accumulate or are removed during growth of ice wedges (figure 4.5b-c). Accumulation of sediments control growth of syngenetic ice wedges which can reach a depth of several tens of meters (e.g., *Yershov*, 2004, p. 323) and grow mainly in vertical direction.

4.1.3. Development of Networks

More or less regular patterns associated with permafrost and related processes within the active layer of permafrost areas are usually termed *patterned ground* (*Embleton and King*, 1975; *Washburn*, 1970). This term lacks any specific genetic implication and comprises not only formation of ice-wedge polygons but also formation of stone-sorting polygons, frost heaving, desiccation, rill erosion and processes described in more detail by *Washburn* (1956, 1970). Patterned grounds produced by ice wedges and thermal contraction fractures are generally addressed as *ice-wedge polygons* or *tundra polygons*.

Polygons form through the interconnection of fractures which occur predominantly at right angles thus forming tetragonal polygonal patterns of intersecting fractures. There are several theories discussing the development of fracture patterns, the first was introduced by *Lachenbruch* (1962, 1966) and *Grechishchev* (1970). According to the theory of *Lachenbruch* (1962, 1966), polygonal cracks show a preferred tendency to orthogonal patterns although there are theories of other workers who consider hexagonal intersection patterns as dominant (*Leffingwell*, 1919; *Black*, 1952). There are indications that fractures forming polygons with hexagonal intersection patterns initiate at randomly distributed points and they subsequently intersect at angles of 120°. In contrast to this, random orthogonal patterns develop when secondary cracks subdivide a fractured area into smaller cells. The term of oriented orthogonal polygonal fracture patterns was introduced by *Lachenbruch* (1966). They form predominantly in the vicinity of bodies of water due to changes in the thermal properties of the ground. This also agrees with the idea that random

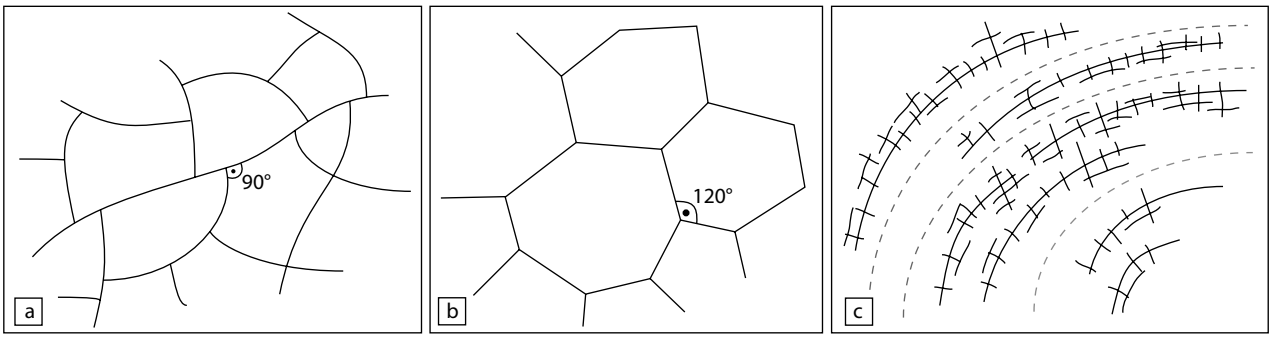

Figure 4.6.: Nomenclature of polygonal network patterns, [a] random orthogonal fracture pattern, [b] hexagonal pattern, [c] oriented orthogonal pattern as often observed at shorelines and river plains, modified after *French* (1996).

orthogonal features develop in heterogeneous material whereas hexagonal fracture patterns develop preferentially in homogeneous material.

According to *French* (1996), p. 94, polygon diameters are usually in the range of 15-40 m. It has been put forward by *Dostovalov and Popov* (1966) that the size of polygonal patterns might be controlled by the severity of climate (*French*, 1996, p. 95). During warmer periods, rectangular polygons form by primary and secondary fissures that are subdivided into many smaller cells during more severe winters. A view that is partly confirmed by *Yershov* (2004) by suggesting that large temperature gradients cause polygonal networks to become smaller. Measurements by other workers indicated, however, that this simple hierarchic concept cannot be observed in the field and polygon development is limited by vegetation and snow cover (*Mackay*, 1986). *Lachenbruch* (1962) estimated on the basis of stress-relief estimates that diameter sizes of polygons depend on the crack depth and that they are usually twice as large as the depth of the crack.

Characteristic of many polygon fractures are raised rims or ramparts which can reach a height of up to 1 m, delineating the troughs (*Mackay*, 1980). Their formation is connected to the growth of ice wedges during which material is deformed and bends upward. It has been suggested, however, that the upturning strata is caused by movement of active-layer material from the center of a polygon towards the trough rims by expansion of the active layer and shearing processes at the boundary of permafrost and the active layer (*Mackay*, 1980).

There are many open questions regarding fracturing and formation of ice-wedges. It is still not completely known, what exactly controls and prohibits reactivation of cracks (vegetation might play a role in this process). Tthere is still much confusion about the interaction concerning creep of the insulating active layer and formation of ridges at either side of frost cracks. Further unanswered questions comprise formation processes of frost-crack networks and the role of high- and low-center polygons. It has been pointed out by *Mackay* (1992) that the theory on frost cracking by *Lachenbruch* (1962) deals with homogeneous media and uniform conditions only whereas the reality is quite different and influencing factors such as relief, climate, material and development of polygons as well as vegetation and snow cover cause uncertainties that can only be addressed through "probabilistic approaches" (*French*, 1996, p. 93).

Modeling attempts over a wide range of climatic conditions have been carried out by *Plug and Werner* (2001, 2002) who inferred that short periods of severe cooling influence the spacing of fractures as well as the frequency. They concluded finally that wedge spacing and width in polygonal networks are controlled by episodes of rapid cooling rather than average conditions. The work by *Plug and Werner* (2002) was, however, considered as not being representative for polygon formation because only epigenetic

types have been modeled that cover only the minority of polygons observed in the field and also produced polygon types that do not exist at all (*Burn*, 2004).

4.2. Martian Polygonal Patterns Indicative of Thermal Contraction Processes

4.2.1. Separation of Landforms

Small-scale polygonal features on the Martian surface have been discovered for the first time with the help of Viking Lander camera observations at the rims of the Utopia Planitia basin. Contemporary to this, an abundance of large-scale polygons in the kilometer-diameter range have been observed in Viking-Orbiter imagery. Although these large-scale features have initially been interpreted as possible thermal contraction polygons, this view has become unpopular. Although their formation is still not completely solved they are not considered anymore as polygons similar to those observed in terrestrial periglacial environments. It became clear that the thermal stresses necessary for formation of polygons of such sizes can not be induced through fluctuations in surface temperatures and the sizes are not consistent with crack-depth estimates necessary for stresses relaxation. Taken into account the coefficient for thermal expansion of ice at temperatures common on Mars (figure 4.2), cracks would not be observable in Viking Orbiter image data (*Hiesinger and Head*, 2000). Consequently, thermal contraction cracking as a process to explain formation of the so-called giant polygons on Mars can be ruled out.

The theories put forward for formation of the Martian giant polygons thus far covered a variety of aspects, some of them are now considered to be obsolete: [1] floor uplift of the Utopia basin caused by either removal of a northern-hemispheric standing body of water, or by freezing and subsequent expansion of residual and buried water, or by a combination of these mechanisms (*Hiesinger and Head*, 2000). [2] loading of sediments (*Helfenstein and Mouginis-Mark*, 1980) or drape folding of a sedimentary cover deposit (*Buczkowski and McGill*, 2002), [3] convection (*Wenrich and Christensen*, 1993), [4] coalescence of small-size polygons (*Helfenstein and Mouginis-Mark*, 1980), [5] tectonic processes (*Mutch et al.*, 1976; *McGill and Hills*, 1992), [6] desiccation (*Morris and Underwood*, 1978), [7] cooling of lava flows as discussed by *Masursky and Crabill* (1976); *Carr et al.* (1976) and *Morris and Underwood* (1978) (as cited in *Hiesinger and Head* (2000)), [8] thermal contraction (*Carr and Schaber*, 1977; *Lucchitta*, 1981; *Jöns*, 1985). An extensive review and summary on the formation of those polygons were provided by *Hiesinger and Head* (2000) and the reader is referred to this work and the references cited herein fur further details.

In contrast to such large polygons, small-scaled features on Mars have a strong morphologic and geometric resemblance to thermal-contraction polygons in terrestrial permafrost although there is still some lack of evidence as some of these crack patterns compare closely to desiccation cracks or even cooling joints in basaltic lava. The problem has not been solved thus far and will probably not be solved until new in-situ observations will reveal the presence of ice- or sand wedges. In earliest work, Viking Orbiter and Lander observations (figure 4.7) of small-scale polygons were interpreted as ice-wedge analogues (*Mutch et al.*, 1977; *Lucchitta*, 1981; *Lucchitta*, 1983). These locally confined observations were expanded with new data from the high-resolution Mars Orbiter Camera (figure 4.8) (*Malin et al.*, 1992; *Malin and Edgett*, 2001). Although the instrument was operating for ten years and has sent almost 100,000 high resolution images back to Earth, the list of contributions published on the topic of thermal contraction cracks and polygons is relatively short with only a small number of full peer-reviewed papers. Most work has been focused on mentioning the morphologic similarity of such features and few papers only report on in-depth observations and analyses.

4.2.2. General Characteristics

Based upon analyses of MOC high-resolution image data, small-scale polygons on Mars have a diame-

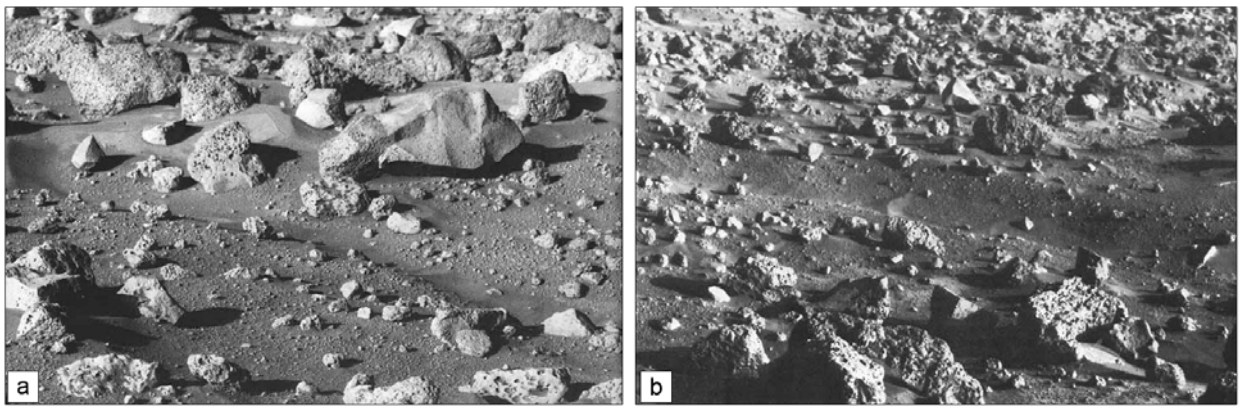

Figure 4.7.: Polygonal network trench observed at Viking Lander 2 landing site (west of crater Mie, 48.27°N, 134.9°E) and which is part of a more extensive polygonal network, interpreted as possible thermal contraction polygon; trench has a depth of 10-15 cm, scene [b] is in the east of scene [a], non-overlapping scenes; (*Viking Lander Imaging Team*, 1978, figures 100 & 104).

ter range of approximately 10-200 m and were separated into two classes: While *Yoshikawa* (2000) and *Paepe et al.* (2001) classified them roughly into one group with polygon diameters of <15 m and one group with polygons having a diameter between 100-200 m, *Mangold* (2005) preferred a class boundary at 40 m. However, statistical arguments for such a size classification have not been provided.

The overall diameter-sizes vary considerably; values range from 20-200 m with an average of 80-90 m (*Kuzmin et al.*, 2002; *Kanner et al.*, 2004) to 10-250 m with an average value of 50 m (*Seibert and Kargel*, 2001). For the south polar regions, diameter values for polygonal fracture patterns are 10-50 m and 100-200 m (*van Gasselt et al.*, 2003b) and range up to 300 m (*Mangold*, 2005).

Crack troughs are generally 4-10 m wide but lower widths also occur (*Seibert and Kargel*, 2001; *van Gasselt et al.*, 2005). Most of the polygons in mid-latitudes are orthogonal in shape and appear as relatively pristine features suggesting a young age (*Seibert and Kargel*, 2001; *Kuzmin et al.*, 2002) although various forms of degradation seem to exist according to *Kuzmin and Zabalueva* (2003). The polygonal features are interpreted as thermal contraction polygons due to their strong resemblance to terrestrial features and have been described for the first time in more detail from the Utopia Planitia rim. A plethora of morphometric values have been extracted by *Yoshikawa* (2000, 2002). Unfortunately, little is known about the intent or the definition of certain values so it can just be assumed on their work that morphometric feature extraction led to the result that polygonal features on the Earth and Mars are comparable. An abundance of morphologic classification work has been performed thus far, separating different erosional and morphological classes but only little light could be shed on the conditions of formation and the topographic control (e.g., *Kuzmin and Zabalueva*, 2003; *van Gasselt et al.*, 2003b; *Mangold*, 2005).

4.2.3. Global Distribution of Polygons

4.2.3.1. Mid-Latitudes

When MOC image data became available, several authors concentrated on the global distribution of polygons on Mars (*Seibert and Kargel*, 2001; *Kuzmin and Zabalueva*, 2003; *Mangold et al.*, 2003). With new data becoming available from Mars Global Surveyor every six months, the density of mapped polygons became higher over the years. First mapping efforts showed some polygons at mid-latitudes and high concentrations of polygons at the Utopia Planitia rim (*Seibert and Kargel*, 2001). This distribution was confirmed in

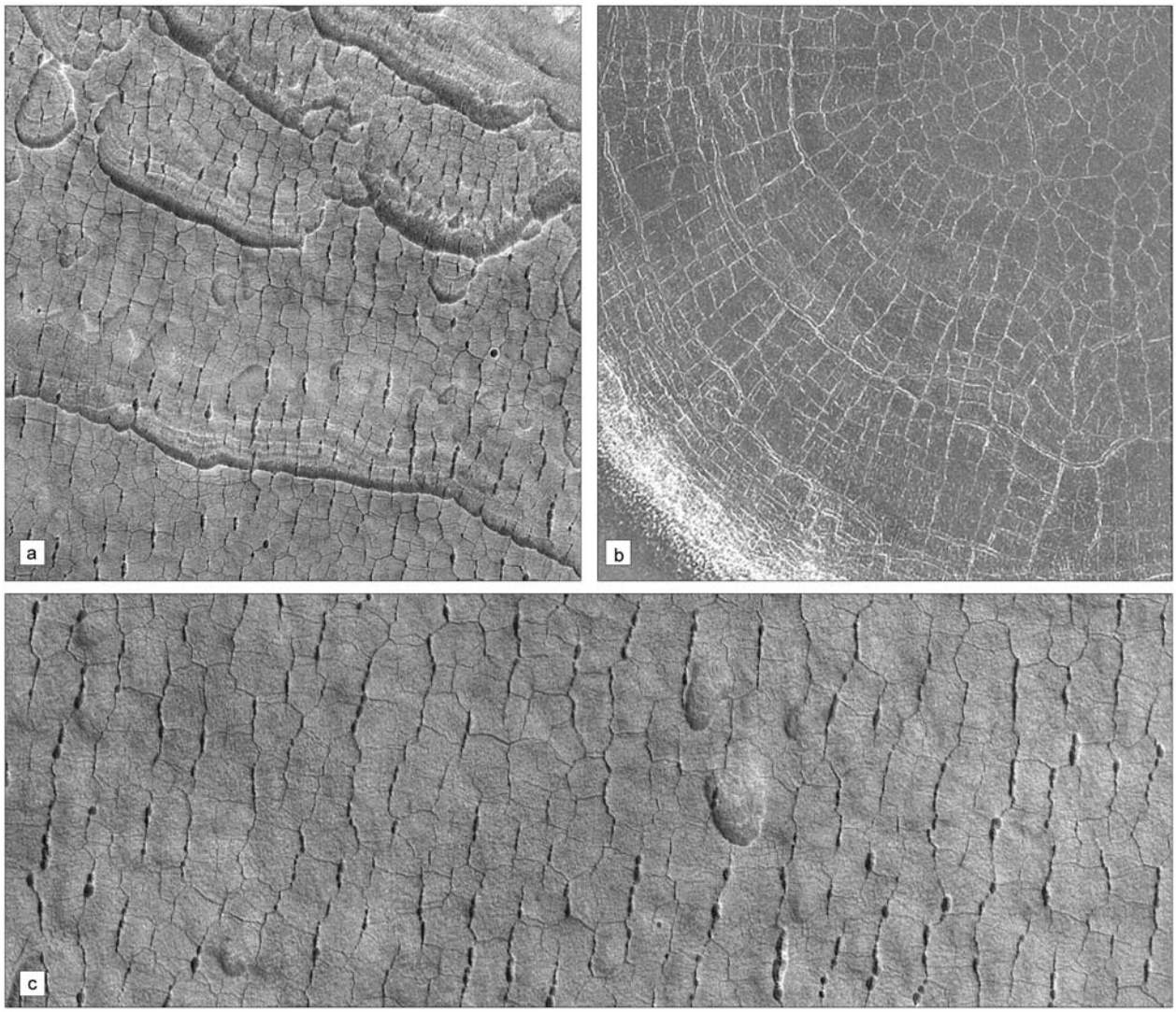

Figure 4.8.: MOC-image samples and types of polygons in Martian mid latitudes; [a] MOC2-1592, 83.9°E, 45.0°N, scene width is 3.0 km, illumination from the lower left; [b] MOC2-426, 32.3°E, 65.6°N, scene width is 2.6 km, illumination from the upper right; [c] MOC2-536, 84.6°E, 45.0°N, scene width is 3.0 km, illumination from the lower left (Malin Space Science System).

later work by *Kuzmin and Zabalueva* (2003) on the basis of new data and also by *Mangold et al.* (2003) (figure 4.9). According to *Mangold et al.* (2003), polygons are distributed polewards of 55° in both hemispheres. The distribution as mapped by *Kuzmin and Zabalueva* (2003) showed that polygons are confined to two latitude belts, one is located between 50°-80°N and the other one is located between 60°-85°S. Both maps provided by *Mangold et al.* (2003) and *Kuzmin and Zabalueva* (2003) show several discrepancies. One major difference is that *Mangold et al.* (2003, 2004) did not include the southern Utopia Planitia polygons in their mapping effort. Reasons for this are that these polygons do not occur within a representative context or they are possibly different in shape or their occurrence was too sparse (*Mangold et al.*, 2003, 2004) (figure 4.9). Mapping of that particular area performed by the author on the basis of the S10 MOC release in 2006 shows a dense distribution of MOC-NA images with polygonal features at the the Deuteronilus area (figure 4.9a) and at the western rim of Utopia (figure 4.9b). Polygons ex-

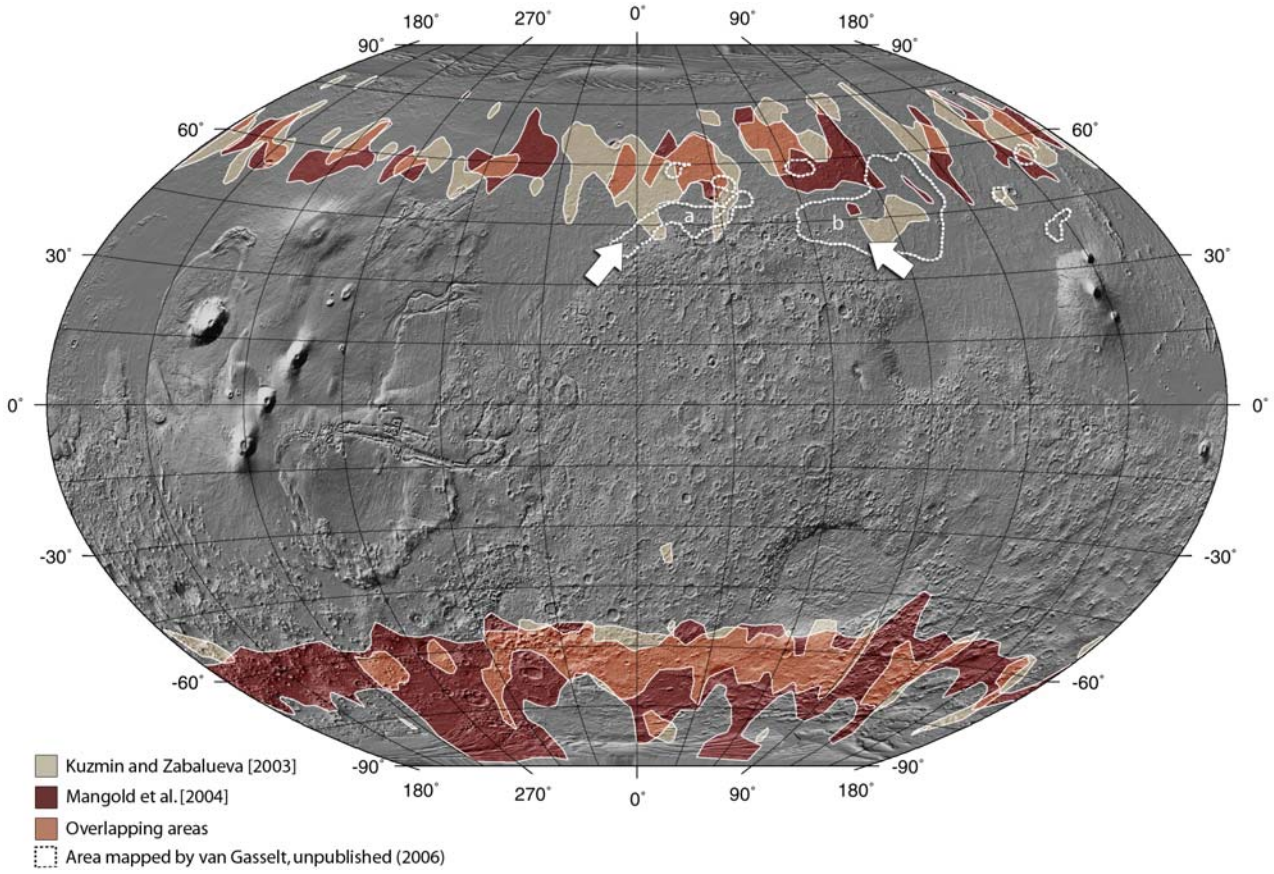

Figure 4.9.: Global distribution of Martian small-scale polygons according to *Mangold et al.* (2004) and *Kuzmin and Zabalueva* (2003). While mapped areas of the southern hemisphere are identical in principle, areas of the northern hemisphere do not necessarily overlap. Arrows mark location of considerable disagreement (see explanation in main text). Maps from publications by *Mangold et al.* (2004) and *Kuzmin and Zabalueva* (2003) have been digitized and reprojected; distributions of polygons were interpolated and conservatively combined to maintain the correct impression; dotted lines mark boundaries of mapping performed by the author on the basis of all available MOC-NA images available in 2006. From these 7600 images located between 0-360°E, 30-60°N, 363 scenes show a polygonal network. Some of them extend farther to the south (location a and b) than suggested by *Mangold et al.* (2004) and partly by *Kuzmin and Zabalueva* (2003).

tend down to 40°N as partly confirmed by mapping of *Kuzmin and Zabalueva* (2003) in Utopia. Work by the author is currently in progress in order to investigates the southern polygons to identify differences in morphology and preservation. This way information is obtained in how far these polygons might also be indicators of changing climatic conditions (see chapter 12, p. 183 for analog studies on debris aprons).

A few confined areas, especially Utopia Planitia and the South Polar region, have been investigated in more detail by some authors recently. *Levy et al.* (2005) as well as *Sletten et al.* (2003) made some comparisons with terrestrial analogy sites in Antarctica. *Sletten et al.* (2003) derived maturation phases that reflect the development of sand-wedge polygons on scales of one million years. Their comparisons showed that "the spacing between adjacent polygon shoulders increases with time along with the width of the sand-wedge". Ongoing development of polygons results finally in growth and formation of a regular pattern of hexagonal polygonal types on timescales between 1 ka to 1 Ma (*Sletten et al.*, 2003). Other regional work comprises the Athabasca Valles area (*Burr et al.*, 2005) and northwest Utopia Planitia (*Soare et al.*, 2005) in which not only polygonal landforms but also pingo features have been possibly iden-

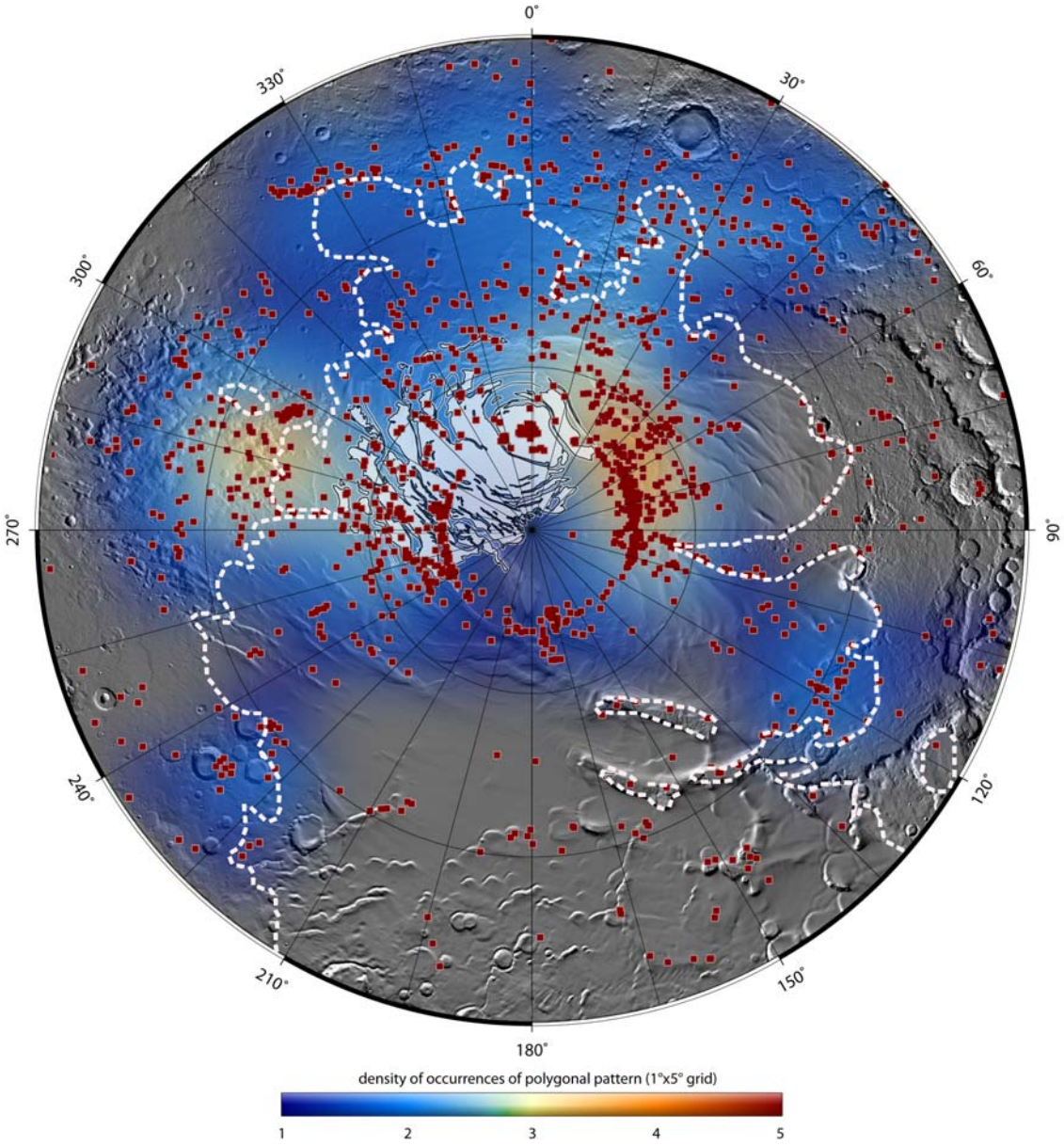

Figure 4.10.: Iso-density representation of the distribution of south-polar polygons, see *van Gasselt et al.* (2003b); *van Gasselt et al.* (2004) and discussion as well as detailed classification in part III, chapter 8, p. 109 and figures 8.15 and 8.14. Dotted white line marks the outer boundary of the south-polar layered deposits (SPLD), red squares mark location of detected polygons, white area near center is the residual polar cap; iso-density calculated on a 1°×5° search grid.

tified.

Age determinations have been conducted on the basis of context estimates: *Mangold et al.* (2003) observed that all polygons that were mapped occur on basically all stratigraphic units but are situated in a young ice-rich mantling described by *Tokar et al.* (2002). A young age was furthermore suggested by the lack of any large impact craters. This way, for most of the mid-latitude polygons ages as young as <10 Ma could be estimated (*Mangold*, 2005). *Seibert and Kargel* (2001) also noticed that polygons appear relatively pristine and are therefore relatively young and are often connected to so-called scalloped depressions interpreted as thermokarst features (*Costard*

and Kargel, 1995). They suggested furthermore that an ice-wedge model is more likely than a desiccation model due to the association with other landforms indicative of permafrost (*Leverington*, 2003).

4.2.3.2. South Polar Area

Apart from the Martian mid-latitudes, a focus was also put on the circum-south polar distribution of polygonal patterns (*van Gasselt et al.*, 2003b; *Mangold*, 2003; *van Gasselt et al.*, 2005; *Mangold*, 2005) (figures 4.10, 8.15 and 8.14). It has been seen early that the south-polar polygons are morphologically different from their mid-latitude counterparts (*van Gasselt et al.*, 2003b; *Mangold*, 2003, 2005). The abundance of polygons at the south-polar cap (figures 4.10, 4.11) and lack of any polygon features near the north pole suggest that their formation might be connected to residual CO_2-ice which is not available at the north polar area. The existence of water and carbon dioxide ice at the south-polar cap might imply that the formation of polygonal terrain is connected also to ice-wedge formation. This has, however, not been supported by observations as the only seasonal observations that have been performed (*van Gasselt et al.*, 2005) have shown that ice-wedge formation is unlikely if such patterns vary from year to year or if the layer in which polygons form is removed. Details on this work are provided in chapter 8, p. 109. The role of CO_2 was also shortly discussed by (*Kuzmin et al.*, 2002) and was considered as possibly important factor in the development of thermal contraction cracks. More specific comments were provided by *Mangold* (2003), suggesting that the extremely long and narrow troughs at the south pole might be caused by the CO_2 cover which reduces the subsurface temperature considerably when it is deposited over circum-south polar areas. Consequently, such a specific morphology of polygonal networks is created (see also *Langsdorf and Britt* (2005)) which might also be an indicators for the former extent of the south polar cap (*Mangold*, 2003).

The dense distribution of south polar polygonal features currently leads to more detailed observations at confined regions. A location that shows a distinct polygonal-network morphology which is probably controlled by underlying topography is found at the Cavi Angusti area and was investigated in more detail (*van Gasselt et al.*, 2006).

Kossacki and Markiewicz (2002); *Kossacki et al.* (2003) finally, investigated the distribution of CO_2 in south polar polygonal troughs and could determine the distribution and mass of subsurface H_2O ice in the regolith with the help of thermal conductivity estimates.

4.2.4. Implications for Ground–Ice

Almost all observations and interpretations of small-scale polygonal terrain on Mars have shown that such landforms might be connected to ground ice. Besides the speculative connection based on morphology, several authors have connected data from the Mars Odyssey Neutron Spectrometer and the derived abundance of hydrogen in the near subsurface to the distribution of polygons. *Kuzmin et al.* (2003) noticed a strong correlation between the mid-latitude distribution of polygons and epithermal and fast neutron-flux deficits that are interpreted as high hydrogen contents in the subsurface (e.g., *Feldman et al.*, 2002; *Mitrofanov et al.*, 2002; *Boynton et al.*, 2002). A similar observation was also made by *Yoshikawa* (2003); *Kanner et al.* (2004); *Soare et al.* (2005) for the circum-Utopia region. However, according to *Yoshikawa* (2002, 2003), Martian polygons at the rims of Utopia are probably not connected to thermal contraction processes but have a tectonic origin and are related to the Hellas Planitia basin. Still he cannot rule out strictly thermal contraction or desiccation processes. The good correspondence between the distribution of polygons and abundances of subsurface hydrogen was confirmed also by *Mangold* (2003); *Mangold et al.* (2004); *Mangold* (2005).

Mangold (2003) considered the distribution of polygons in the southern hemisphere and the correspondance to the distribution of subsurface hydrogen as detected by Neutron Spectrometer measurements as a convincing argument for the periglacial nature of these features. As seasonal thawing does not oc-

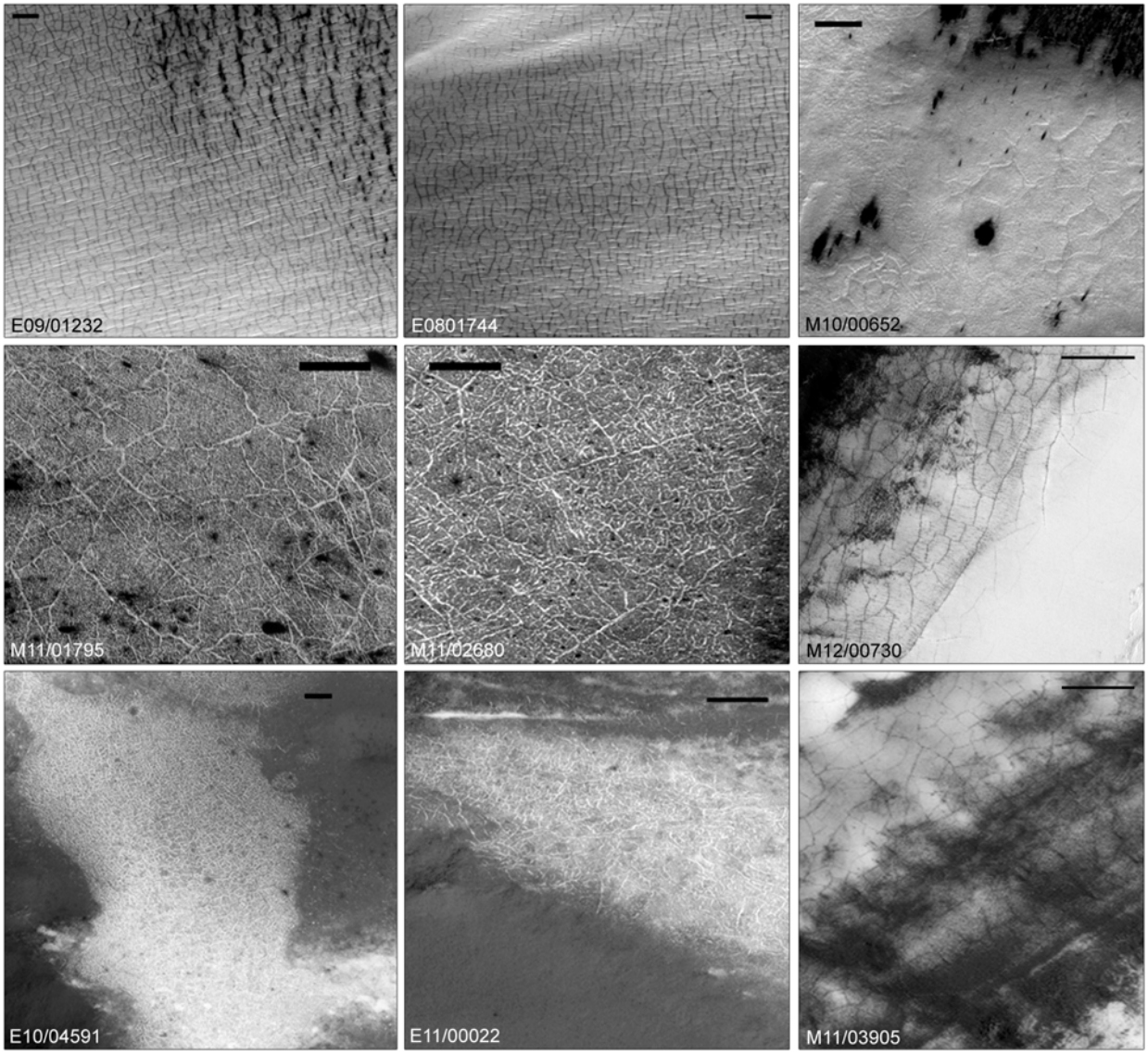

Figure 4.11.: MOC-image samples and types of polygons in the south polar area and the residual carbon-dioxide ice cap; scenes are labelled with MOC-image numbers, bar is 100 m across, see also figure 8.14 (*van Gasselt et al.*, 2003b).

cur on Mars to allow ice-wedge formation, *Mangold* (2003); *Mangold et al.* (2004); *Mangold* (2005) also suggested the possibility of climatic variations in the past. Apart from morphological research, modelling has been conducted by *Mellon* (1997) using data from the Viking Lander 2 landing site. He estimated that thermal stresses occurring at the surface (at a depth of 0.5 m) due to seasonal temperature variations are in the range of up to 6 MPa north of 20-30°N latitude. Such tensile stresses easily exceed the regolith strength of 2-3 MPa and could consequently generate contraction cracks. □